Electronics and Electrical Engineering

http://www.aimspress.com/journal/ElectrEng

AIMS Electronics and Electrical Engineering, 6(1): 1–15.
DOI: 10.3934/electreng.2022001
Received: 23 October 2021
Revised: 24 December 2021
Accepted: 06 January 2022
Published: 13 January 2022

Research article

Genetically engineered tri-band microstrip antenna with improved directivity for mm-wave wireless application

Arebu Dejen[1,*], Jeevani Jayasinghe[2], Murad Ridwan[1] and Jaume Anguera[3,4]

[1] School of Electrical and Computer Engineering, Addis Ababa University, Addis Ababa, Ethiopia
[2] Department of Electronics, Wayamba University of Sri Lanka, Kuliyapitiya, Sri Lanka
[3] GRITS remote-IoT Research Group, Universitat Ramon LLull, Barcelona, Spain
[4] Ignion, Barcelona, Spain

* **Correspondence:** Email: arbdjn@gmail.com.

Abstract: Multi-band microstrip patch antennas are convenient for mm-wave wireless applications due to their low profile, less weight, and planar structure. This paper investigates patch geometry optimization of a single microstrip antenna by employing a binary coded genetic algorithm to attain triple band frequency operation for wireless network application. The algorithm iteratively creates new models of patch surface, evaluates the fitness function of each individual ranking them and generates the next set of offsprings. Finally, the fittest individual antenna model is returned. Genetically engineered antenna was simulated in ANSYS HFSS software and compared with the non-optimized reference antenna with the same dimensions. The optimized antenna operates at three frequency bands centered at 28 GHz, 40 GHz, and 47 GHz whereas the reference antenna operates only at 28 GHz with a directivity of 6.8 dB. Further, the test result exhibits broadside radiation patterns with peak directivities of 7.7 dB, 12.1 dB, and 8.2 dB respectively. The covered impedance bandwidths when $S_{11} \leq$-10 dB are 1.8 %, 5.5 % and 0.85 % respectively.

Keywords: tri-band antenna; microstrip antenna; genetic algorithm optimization; mm-wave antenna

1. Introduction

The rapid growth in mobile device density is an evidence for the increment of the number of services expected from a single device. Concurrently, the paucity of resources such as bandwidth is occurred in the microwave frequency to deliver services with high data rates for the satisfaction of customers [1]. Hence, the wireless communication industry has expanded its spectrum to millimeter wave (mm-wave) frequency, which has adequate bandwidth. In mm-wave wireless applications, the integration of sensing or imaging with wireless communication in a single device is now more prevalent. Existing

communication platforms might be used for sensing with modest changes to hardware, signaling mechanisms, and networking protocols. The incorporation of sensing into today's IoT devices and cellular networks demands the use of a well-designed antenna, which is an essential component of any wireless link.The antenna requires a careful consideration in optimizing, designing, manufacturing and packaging for transmitting sensing and imaging data wirelessly. Especially, the mm-wave signals are agonizing atmospheric fascination and high path loss, thus the outline of mm-wave antenna has two additional concerns; high directivity and expedient size besides with multiband operation [2].

In the arena of wireless application technology, a large number of new users get access via multiple channels, thus there is a need of a prominent development in multiband antennas [3]. It is indispensable for mm-wave mobile terminal antennas to have a low profile and a low budget in order to have the peculiarity to work at distinct mm-bands. An antenna with high potential to fulfill the anticipated condition is the microstrip patch antenna. In spite of its narrow bandwidth and low gain, microstrip patch antenna has many benefits, like easy manufacturing, low profile, less weight and planar structure [4]. The majority studies related to directivity improvement of microstrip patch antenna are linked to patch arrays [5, 6]. However, the antenna's performance is hampered by the intricate array feeding network, the antenna size, and mutual coupling. As a result, researchers suggested a variety of methodologies and optimization strategies for improving antenna directivity and expanding multi-functionality while avoiding the convoluted feeding network [7–9].

For multi-band antenna optimization, bio-inspired algorithms such as genetic algorithms, differential evolution, wide drive, invasive weed, particle swarm, ant colony, and bacterial foraging algorithms are used for various application [10–12]. Genetic algorithm is the progression of hereditary assortment in which the fittest individuals are selected for cloning of offsprings for the next generation. It is a stochastic optimization method that has been used to solve electromagnetic optimization problems over the last two decades. The algorithm doesn't require a derivative solution and a prior knowledge about the problem. It can also handle more complex problems than the other most commonly used antenna optimization algorithms, such as particle swarm optimization (PSO) [13].

Innumerable mechanisms have been reported in the literature to develop multiband mm-wave microstrip patch antennas for wireless network in imaging and sensing application which require multi-spectrum operation from a single device. Particle swarm optimization was used to obtain ideal patch size and slot positions on the patch surface, resulting in multi-frequency resonance of the patch antenna [14–16]. To achieve multiband operation, directivity improvement, and bandwidth enhancement, genetic algorithm optimization was also used for feed position investigation, patch geometry optimization, appropriate patch dimension, and proper discovery of placements of shorting pins [17–19]. Alternative techniques such as slot, slit, or a loading stub on one of the patch antenna structures viz. radiating patch, substrate, or ground plane were employed to enhance multi-functionalities of antenna [20–25]. As far as the authors knowledge there is no work conducted on antenna optimization using genetic algorithm for triple-band service and directivity improvement at mm-wave frequency.

To develop a tri-band mm-wave antenna with better directivity, this research presents binary coded genetic algorithms. The technique is optimal for maintaining the surface of a radiating patch. The radiating patch's surface is partitioned into 10×10 small rectangular cells, with conducting and non-conducting attributes assigned to each. Instead of establishing a predefined patch geometry, an iterative genetic algorithm approach returns a novel model of the radiating patch while preserving the

optimal substrate height and antenna size. The approach simplifies the antenna structure, lowering its complexity and residual radiation while improving the antenna's directivity and multi-functionality. A non-optimized reference antenna is compared to a genetically altered antenna in the study. Except for the morphologies of patch geometry, which are segmented into small rectangular cells in the optimized antenna by the optimizer, both antennas have equal dimensions.

2. Antenna configuration

In this article, a rectangular patch microstrip antenna with microstrip line feeding has been considered. Besides the feeding line, the antenna comprises three strata viz. a radiating patch, a ground plane and substrate [26]. In the reference antenna design, the finite ground plane is made of copper having a dimesion of $L_s x W_s$ was employed. The selected substrate material is FR4-epoxy with thickness of 0.6 mm, dielectric constant 4.4, and loss tangent 0.02 in the size of ground plane due to its availability and affordability. The research has been started with a conventional microstrip patch antenna design which resonates at center frequency of 28 GHz. The maiden suboptimal dimensions of microstrip antenna were computed using the governing standard design formulae presented in [27]. A proportional modification has been done on dimensions to obtain an adequate antenna performance at a proposed center frequency using parametric analysis. The analysis was carried out to determine reference antennas optimal dimension by a possible decreasing of reflection coefficient at the resonating frequency (28 GHz). The engagement of a specific antenna variable is investigated at a time, while all other parameters are maintained at sub-optimal values in the computation. The length of the patch dimension was varied from 3.8 mm to 4.6 mm in five stages, while the width of the patch was varied from 6.2 mm to 7.0 mm with a 0.2 mm gap to get the ideal value of 4.4 mm length (L_p) and 6.6 mm width (W_p).

The rectangular patch antenna is fed by a characteristics impedance of 50 ohm microstrip line feeder with a total feed length of 3.3 mm and a width of 0.7 mm. The feed-line width is constructed in three segments for input impedance matching, and the starting width of the feeding line is 0.7 mm. Figure 1 shows the final model of a proposed reference rectangular microstrip patch antenna that is ready for patch shape optimization, and Table 1 summarizes the optimal dimensions of antenna parameters

Table 1. Summary of dimensions for the referenced antenna model.

Parameter	substrate			Patch		Feed line	
	Length (L_s)	Width (W_s)	Thickness (h)	Length (L_p)	Width (W_p)	Length (L_f)	Width (W_f)
Value	8.2 mm	10.2 mm	0.6 mm	4.4 mm	6.6 mm	3.3 mm	0.7 mm

Since the aim of this research is to develop a tri-band patch antenna with enhanced directivity, genetic algorithm optimization is applied on the patch surface in order to create various current paths that will assist the antenna to attain multiple resonating mm-wave frequencies.

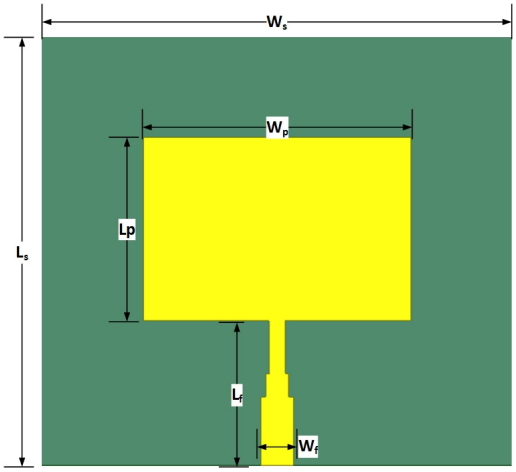

Figure 1. The front and perspective view of reference microstrip patch antenna on finite ground plane and substrate thickness h = 0.6 mm, ϵ_r = 4.4, and tanδ = 0.02.

3. Genetic algorithm procedure

To perform a binary coded genetic algorithm optimization, the reference antenna's patch surface is partitioned into 10 × 10 uniform small rectangular cells. Each chromosome in the population is represented by 100 genes. The first generation was twisted at random, and subsequent generations are made up of more fit individuals depending on the cost function's scrutiny. As shown in the flow chart Figure 2, genetic algorithm operators like crossover, mutation, and selection are employed iteratively until the termination requirement is met. The method may be used to optimize antennas in a range of applications, including wireless communication, IOT application, and wireless sensor networks. As a consequence, genetic algorithms might be employed to increase the performance of antennas used in data transmission from various monitoring scenarios, such as sensing and imaging for industrial and medical applications.

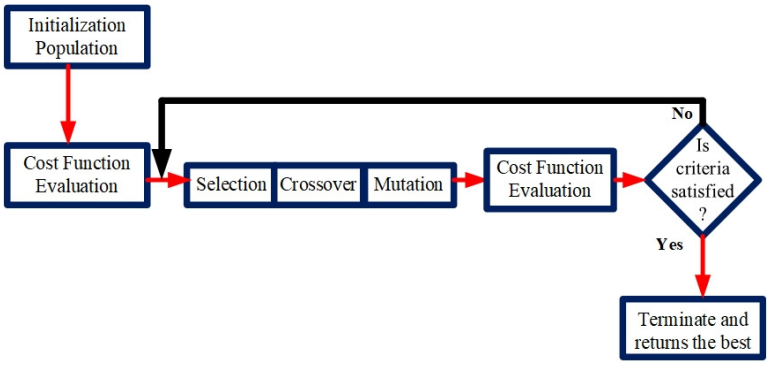

Figure 2. Genetic algorithm flowchart.

In order to avoid infinitesimal points contacting each other at the corner of a cell, overlapping was done by shifting cell dimensions as illustrated in Figure 3(b). The size of a rectangular cell is 0.44 mm x 0.66 mm and the overall pattern of the gridded patch surface is presented in Figure 3(c).

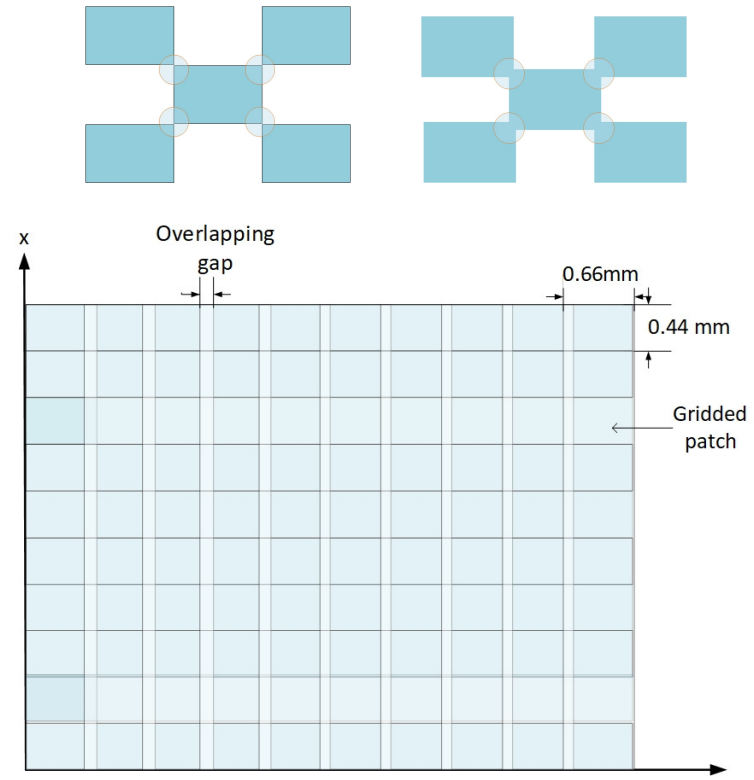

Figure 3. (a) Conventional infinitesimal connections(magnified) (b) Suggested cell overlapping outline(magnified), (c) cell distribution on the patch surface.

A binary coding algorithm defines the conductivity feature of each cell. For conducting surfaces, the cell is assigned gene '1' and for non-conducting surfaces, gene '0'. The optimization procedure is performed on each individual's radiating patch geometry, which consists of 100 genes. A gene can only exist in one of two states: "on" or "off." The gene '0' represents the "off" state of the cell, indicating that it is non-conducting, and the optimizer removes non-conducting cells from the radiating patch surface. Gene '1', on the other hand, represents the active cells of the radiating patch, which will be preserved as part of the individual antenna.

Over the iterations, the optimization method use a combination of MATLAB and HFSS software. A MATLAB code designed to generate a visual basic Script (VBS) files that contains the details of a proposed antenna and HFSS calls each VBS file to model and compute the far-field and near-field antenna parameters [28]. After modeling and computing each aspirant solution (individual) in HFSS, genetic algorithm optimizer code continues to evaluate the fitness function in MATLAB. The process endures until the end of the iteration or the termination criterion is reached, as shown in Figure 4(a). In this article, chromosomes were encoded using a single level binary string representation approach. The population of a generation G is represented by a variable P, and the original population was chosen at random. The remainder generation reproduction and selection procedures were carried out in accordance with the description of Holland's schema theorem [30]. The MATLAB model of the algorithm is summarized by a simple pseudo-code given in the Figure 4(b).

One of the main goals of this optimization is to improve the broadside directivity and achieve the best possible reflection coefficient of the antenna at three different frequencies. As a result, the fitness

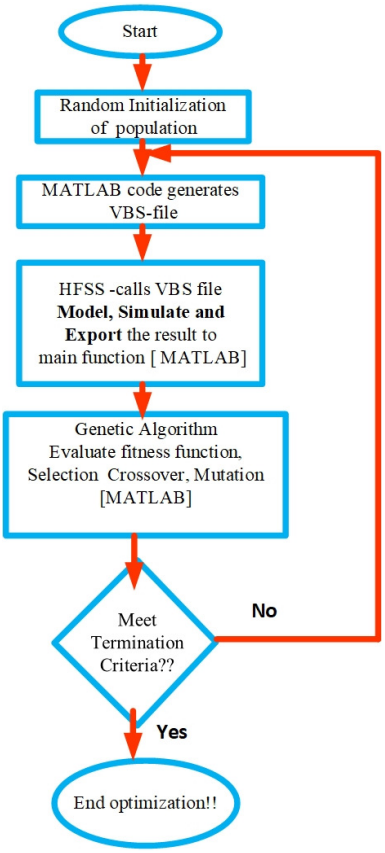

Algorithm-1: Pseudo code representation of the main function in MATLAB

```
1:  begin
2:     G=0
3:     Random initialization P(G)
4:     Evaluate the fitness value of P(G)
5:     While not satisfy
6:        do
7:           begin
8:           G=G+1
9:           Select P(G) from P(G-1)
10:          Reproduce pairs in P(G)
11:          Evaluate P(G)
12:          end
13:    end
```

Figure 4. (a) Block diagram for MATLAB and HFSS interface in genetic algorithm antenna optimization (b) Pseudo code for Genetic algorithm optimization in the main function.

function is defined as increasing the negative sum of the reflection coefficient $S_{11}(f_i)$ and maximizing the directivity $D(f_i)$ over the desired frequency range, as presented Equation (3.1).

$$FitnessFunction = -[\frac{1}{N}\sum_{i=1}^{N}(S_{11}(f_i) - D(f_i)) + \frac{1}{M}\sum_{i=1}^{M}(S_{11}(f_i) - D(f_i)) + \frac{1}{K}\sum_{i=1}^{K}(S_{11}(f_i) - D(f_i))] \quad (3.1)$$

Where
N: total number of sampling points in the first band
M: total number of sampling points in the second band
K: total number of sampling points in the third band
f_i: the sample frequency, the sampling period was taken as 100 MHz
$D(f_i$: directivity of the antenna at sample frequency in dB
$S_{11}(f_i)$: reflection coefficient at sample frequency in dB. Taking $S_{11}(f_i)$ =-10 dB if its value is less than -10 dB, avoids the narrow impedance bandwidth at the center frequency.

$$S_{11}(f_i) = \begin{cases} S_{11}(f_i) & if S_{11}(f_i) \geq -10dB \\ -10dB & if S_{11}(f_i) \leq -10dB \end{cases}$$

The summary of optimization setup is presented in Table 2.

Table 2. Summary of genetic algorithm optimization setup.

No.	Optimization parameter	Values	Remarks
1	Number of cell/genes in a chromosomes	100	10*X*10
2	Population size	30	Individuals
3	Maximum number of generations	200	
4	Crossover type	Single point	
5	Probability of crossover	0.7	
6	Mutation	Single bit	
7	Mutation rate	0.2	
8	Selection Type	Tournament selection	

4. Results and discussion

As previously highlighted, each patch geometry is represented by 100 genes, resulting in 2^{100}= 1.2677 x 10^{30} potential solutions according to the binary coded genetic algorithm. Each individual candidate is modeled and simulated in HFSS with finite element method. The individuals are run through a fast sweep computation from 25 GHz to 50 GHz with a 100 MHz sampling frequency and the far field radiation sphere setup of 0^0-360^0 for both θ and ϕ components in a 10^0 step size. If each simulation takes 1 second to compute, the total computing time to address the whole solution space is 4.02 x 10^{22} years. However, thanks to genetic algorithm, it was able to search the fittest individual from the solution space in 6.25 days using Core-I7 computer with 8GB RAM and processor speed of 2.7 GHz.

On each iteration, the patch cell's (gene in a chromosome) 'on' and 'off' states were maintained. The algorithm evaluates the fitness function and runs its process indefinitely until a new radiating patch model meets the termination conditions. The algorithm's fitness value increases dynamically until convergence is obtained at the 160^{th} generation, as illustrated in figure 5(a). The optimization procedure is carried out until the 200^{th} generation in order to demonstrate the consistency of the fitness value over the next 40 generations. Finally, after 200 generations, the best-fitting individual antenna is returned, as shown in Figure 5(b).

The simulated results of both the optimized and reference antennas are given and compared after optimization is completed. Figure 1 shows a reference rectangular microstrip patch antenna that was simulated and found to resonate at 28 GHz, resulting in a single frequency resonance with a 1.7 % bandwidth, as seen in Figure 6. The directivity of this antenna is 6.8 dB, which is adequate for a traditional rectangular microstrip antenna. However, this is insufficient for mm-wave wireless application. Therefore, optimization was applied to hoist directivity and multi-band operation.

The simulated results depicted that the genetically engineered antenna operates at three distinct frequency bands: 27.8–28.3 GHz, 38.4–40.6 GHz and 46.8–47.2 GHz, as shown in Figure 6. The antenna resonates at center frequency of 28 GHz with peak S_{11} value of -18.8 dB, at 40 GHz with peak S_{11} of -48.1 dB, and at 47 GHz with peak S_{11} of -26.89 dB. When considering $S_{11} \leq$ -10 dB, the bandwidth augmentation of the antenna has been visualized when compared to the reference model and previously stated antennas. It is delineated that the impedance bandwidth is realized 500 MHz at 28 GHz, 2.2 GHz at 40 GHz, and 400 MHz at 47 GHz. The improved antenna's entire operating

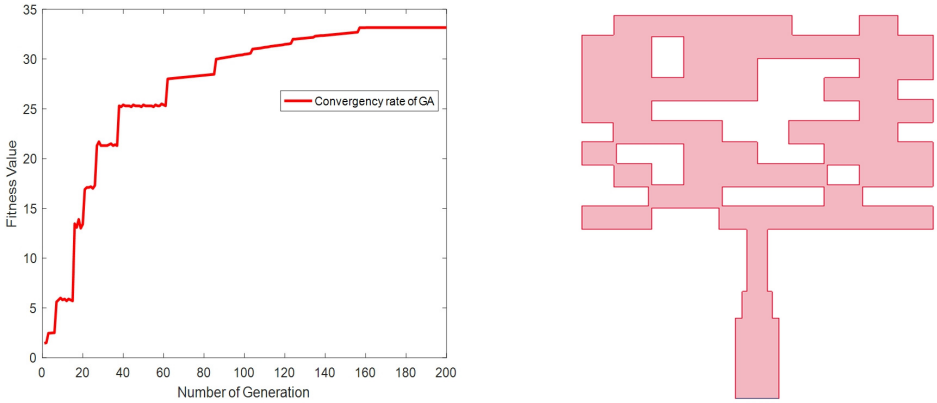

Figure 5. (a) convergence rate of genetic algorithm and (b) The best fitted individual patch antenna structure.

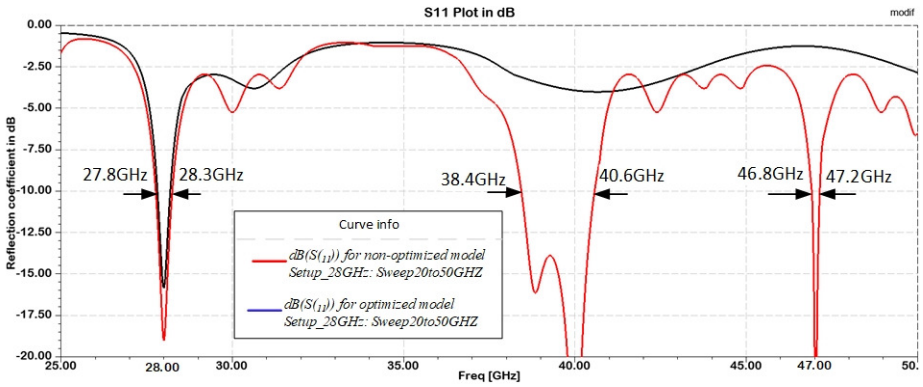

Figure 6. Simulated S_{11} results of both reference model and genetically optimized antenna.

bandwidth is 2.7 GHz higher than the reference antenna which is important to transmit huge amount of data at a time with low latency in mm-wave wireless communication. Table 3 shows that the proposed antenna outperformed the reference antennas in terms of reflection coefficient across all operational bands. In the working bands, the optimized antenna has achieved a reflection coefficient that is roughly 1.23 - 3.14 times lower than the reference antenna. The lesser the value of the reflection coefficient, the better the outcome.

The input impedance should be close to 50 Ω according to the specifications of this optimizer. The input impedance of the genetically optimized antenna is 49.69 + j11.29 Ω, 50.23 + j0.41 Ω, and 48.5–j3.85 Ω at 28 GHz, 40 GHz, and 47 GHz, respectively. This shows that how the antenna's input impedance matching level has improved. The conventional microstrip antenna in the reference model has an input impedance of 44.36 – j14.29 Ω at 28 GHz resonant frequency. The antenna's impedance matching is enhanced to this level because the method is utilized to study a lower level of the reflection coefficient.

Furthermore, the antenna's directivity is improved when compared to a conventional antenna. The directivity of a genetically engineered antenna is 1.8 times higher than the directivity of a reference model. When the maximum peak directivity larger than 10 dB is considered, it is observed that the techniques presented in [20] provides the highest directivity in the literature form a single antenna,

however this paper presents 12.1 dB using genetic optimization. As shown in Figure 7(a), which is the directivity versus frequency cut at $\phi = 90^0$ and $\theta = 0^0$, the optimized antenna has a peak broadside directivity of 7.7 dB at 28 GHz, 12.1 dB at 40 GHz, and 8.2 dB at 47 GHz. In mm-wave multi-functional wireless network directivity improvement of the antenna is essential to resist the propagation attenuation in the link. In all three operational bands, the proposed antenna produced a broadside radiation pattern, as shown in Figure 7(b). The pattern in the figure was cut when $\phi = 90^0$ at three distinct resonant frequencies with all theta values. As a result, the optimized antenna has the upper hand in all three operating bands.

Table 3. Performance of reference and optimized antennas.

Antenna	Resonating frequency(GHz)	S11 (dB)	Bandwidth (MHz)	Fractional Bandwidth (%)	Directivity (dB)	Radiation Efficiency (%)
Reference antenna	28	-15.3	480	1.7	6.8	73.9
Optimized antenna	28	-18.8	500	1.8	7.7	62.2
	40	-48.1	2200	5.5	12.1	45.1
	47	-26.9	400	0.85	8.2	61.9

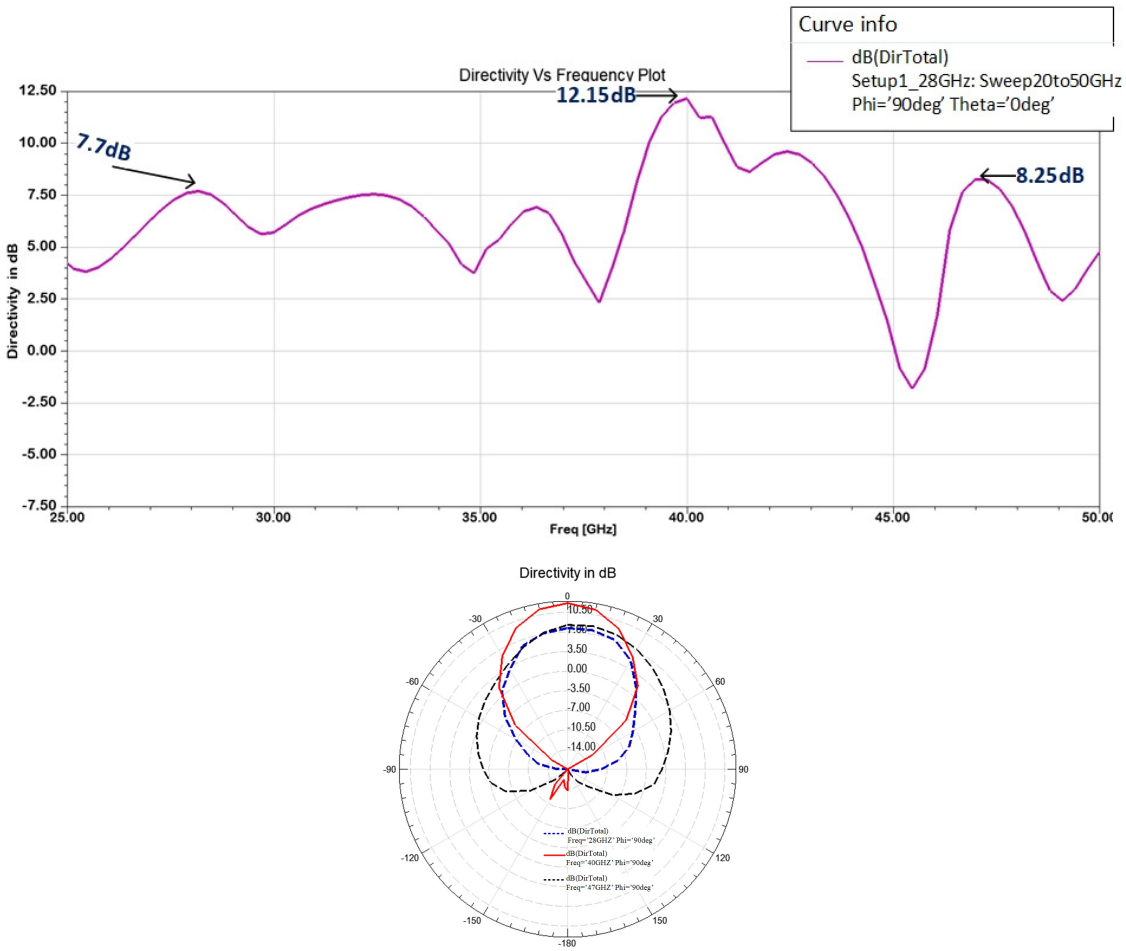

Figure 7. Directivity in dB (a) Versus frequency plot when ϕ=90^0 and θ=0^0, (b) polar plot at three resonant frequency when ϕ=90^0.

Figure 8 shows that a proposed tri-band antenna has a radiation efficiency of 62.2 % at 28 GHz, 45.1 % at 40 GHz and 61.9 % at 47 GHz with a total efficiency, which includes the mismatched loss in consideration, are 61.2 %, 44.5 % and 59.3 % respectively. However, radiation efficiency can be improved by employing low loss dielectric material [27]. For instance, radiation efficiency is enhanced to 90.3 % at 28 GHz, 93.5 % at 40 GHz and 89.7 % at 47 GHz when tanδ = 0.002 is considered.

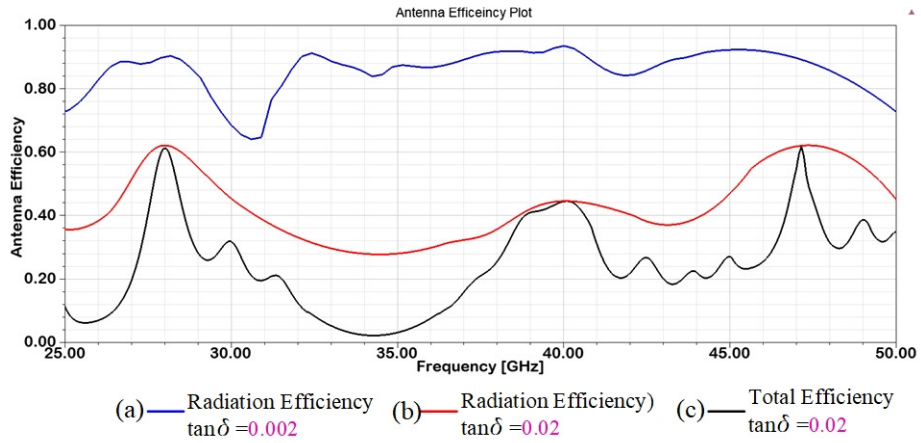

Figure 8. Proposed antenna efficiency plot (a) Radiation efficiency with tanδ=0.002,(b) Radiation efficiency with tanδ=0.02 and (c) Total efficiency with tanδ=0.02.

The antenna also has a gain melioration of 5.6 dB, 8.7 dB and 6.1 dB at 28 GHz, 40 GHz and 47 GHz respectively. The realized gain of genetically engineered antenna at each resonance frequency is presented in Figure 9 in polar plot. As seen from the figure, the pattern has a comparable beam width for both $\phi = 0^0$ and $\phi = 90^0$. The pattern also reveals a null propagation at $\theta = 180^0$ for the two operational bands 28 GHz and 47 GHz. However, at 40 GHz when $\phi = 90^0$, a little back lobe appears. At 47 GHz, the antenna's wider beam width is detectable, but narrow beam width is also visible at 40 GHz. From the far field radiation parameters, it can be seen that the genetically optimized antenna significantly outperforms the reference antenna in terms of the number of operation bands, directivity and gain.

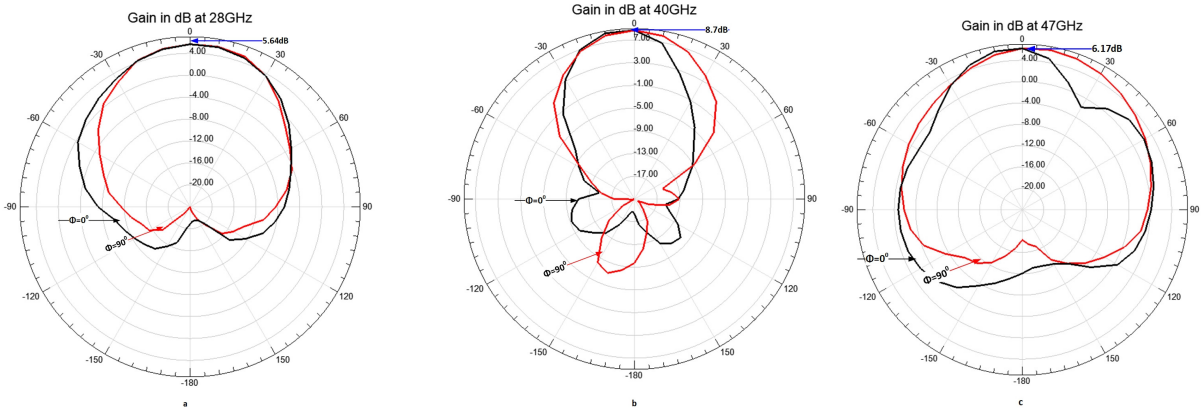

Figure 9. Polar plot of realized gain in dB when phi=0^0 and phi= 90^0 of optimized antenna.

The table below compares the findings of this study to those of other researchers in the literature (Table 4). As indicated in the table's remark section, these papers investigated a variety of techniques to increase antenna performance, while this antenna utilizes genetic algorithm. The proposed antenna able to operate in three distinct bands and compared to a multiband related works. The comparison demonstrates that the proposed work outperforms the rest of the literature more than 2 dB in directivity. The survey also reports that the maximum peak realized gain of a single antenna was achieved by fractal shaped structure is 7.67 dB in microwave frequency range while the gain of the proposed antenna higher than nearly 1 dB in mm-wave frequency. In addition, the antenna has a wide bandwidth in all three working bands when compared to others. The antenna's performance was realized by employing a binary-coded genetic algorithm for patch geometry optimization.

Table 4. Comparison of this paper with related works.

Papers	Patch size in λ^2	Center freq.(GHz)	Fractional Bandwidth (%)	Gain dB	Directivity dB	Remark (/methods)
[4]	0.43 x 0.43	2.6	15	5.42	–	elliptical-shape
		6	14	6.52	-	fractal
		8.2	59	7.67	-	geometry
[15]	1.75 x 1.68	42	11.9	5.8	–	Particle
		51.5	14	3.9	-	Swarm
		60	9.2	5.3	-	Optimization
[17]	0.38 x 0.36	1.98	4.6		8.34	Genetic
		2.65	4.3		8.75	algorithm
		3.19	5.3		7.56	optimization
[20]	0.48 x 0.48	14.66	-	5.44—max	10.06—max	-Inset feed +
		23.25	–	-		- Rectangular
		28.9	–	–		slit
[21]	0.24 x 0.26	11.65	0.8	–	7.41	Position and
		13.96	1.8	–	7.99	size of slit
		17	0.8	–	7.3	optimization
[23]	0.56 x 0.56	28	4.6	7.6	8.5	Elliptical slot
		45	2.2	7.25	7.56	Dual-band
[24]	0.53 x 0.57	23.9	-	4.43	–	Inset feed
		35.5	-	3.66	-	
		70.9	-	5.64	-	
[29]	1.1 x 0.95	25.4	29	6.4	6.9	semi-
		34.6	11.7	5.88	6.3	circular
		38	8.6	7.04	7.5	slot
This paper	0.41 x 0.61	28	1.8	5.64	7.7	Genetic
		40	5.5	8.7	12.15	algorithm
		47	0.85	6.17	8.25	optimization

The surface current distribution of the reference antenna and genetically engineered antenna at the intended frequency is presented in Figure 10. The engineered antenna operates in three frequency bands due to the availability of several current routes on the optimized patch shape. As the figure depicts that the current distribution of the reference antenna at 28 GHz is greater closer to the microstrip line and patch edge. At 28 GHz, the edge of the cells on the left side of the optimized antenna has the highest current distribution, whereas at 40 GHz, the edge of the cells on the right side has the highest current distribution. The current distribution is high on the center and right cells at 47 GHz.

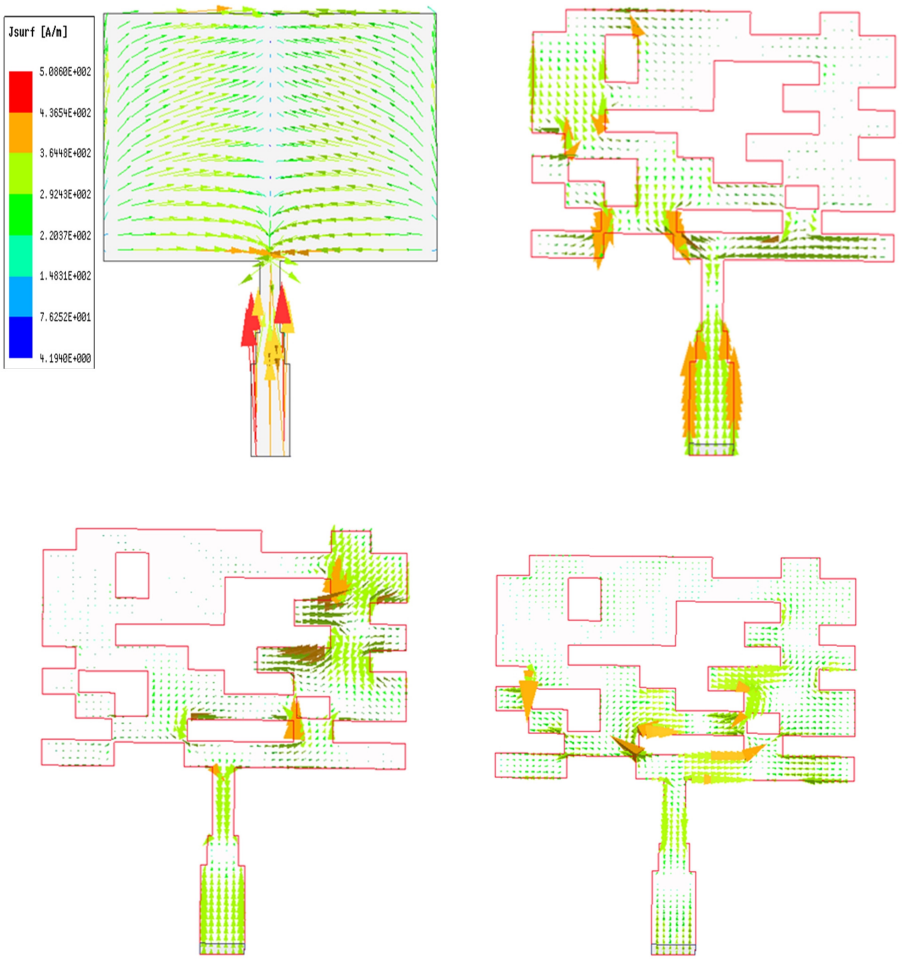

Figure 10. Surface current distribution (a) reference antenna at 28 GHz and optimized antenna (b) at 28 GHz, (c) 40 GHz and (d) 47 GHz.

5. Conclusions

This paper presents optimization of a tri-band mm-wave rectangular microstrip patch antenna using binary coded genetic algorithm. The computations and simulations were carried out by a combination of MATLAB and HFSS. The optimization procedure and strategies were discussed and the results were compared with a reference rectangular antenna. The proposed antenna with binary coded genetic

algorithm provided a triple band operation at 27.8–28.3 GHz, 38.4–40.6 GHz and 46.8–47.2 GHz while the reference antenna operates only at a single band (28 GHz). The tri-band antenna operates at center frequency of 28 GHz, 40 GHz and 47 GHz with the peak directivity of 7.7 dB, 12.1 dB and 8.2 dB respectively. The corresponding total efficiencies of a proposed antenna are 61.2 % at 28 GHz, 44.5 % at 40 GHz and 59.3 % at 47 GHz. In a nut shell, genetic algorithms was applied for optimization of a multiband microstrip antenna to maximize directivity and to minimize return losses at desired frequencies by avoiding complicated feeding system and losses caused by antenna array.

Conflict of interest

The authors declare that there is no interests in this paper.

References

1. Kumar KB, Shanmuganantham T (2017) Multiband E-shape SIW Antenna for mm-Wave Applications. In *IEEE International Conference on Computer, Communication, and Signal Processing ICCCSP-2017*, 1–5.
2. Hakim ML, Faisal M (2019) Design and Simulation of a Multiband Millimeter Wave Microstrip Patch Antenna Array for 5G Wireless Communication. In *22nd International Conference of Computer and Information Technology ICCIT-2019*, 1–5.
3. Roy P, Vishwakarma RK, Jain A, et al. (2016) Multiband Millimeter Wave Antenna Array for 5G Communication. In *International Conference on Emerging Trends in Electrical, Electronics and Sustainable Energy Systems ICETEESES*, 102–105.
4. Kaur A, Malik PK (2021) Multiband Elliptical Patch Fractal and Defected Ground Structures Microstrip Patch Antenna for Wireless Applications. *Progress In Electromagnetics Research B* 91: 157–173. https://doi.org/10.2528/PIERB20102704
5. Dzagbletey PA, Jung YB (2018) Stacked Microstrip Linear Array for Millimeter-Wave 5G Baseband Communication. *IEEE Antenn Wirel Pr* 17: 780–783. https://doi.org/10.1109/LAWP.2018.2816258
6. Rodríguez-Cano R, Zhang S, Pedersen GF (2018) Beam-Steerable Multi-Band Mm-Wave Bow-Tie Antenna Array for Mobile Terminals. In *12th European Conference on Antennas and Propagation (EuCAP 2018)*. https://doi.org/10.1049/cp.2018.0418
7. Jayasinghe JW, Anguera J, Uduwawala DN (2013) A High-Directivity Microstrip Patch Antenna Design by Using Genetic Algorithm Optimization. *Progress In Electromagnetics Research C* 37: 131–144. https://doi.org/10.2528/PIERC13010805
8. Anguera J, Andújar A, Benavente S, et al. (2018) High-directivity microstrip antenna with Mandelbrot fractal boundary. *IET Microw Antenna P* 12: 569–575. https://doi.org/10.1049/iet-map.2017.0649
9. Anguera J, Andújar A, Jayasinghe J (2020) High-Directivity Microstrip Patch Antennas Perturbing $TM_{odd\text{-}0}$ Modes. *IEEE Antenn Wirel Pr* 19: 39–43. https://doi.org/10.1109/LAWP.2019.2952260

10. Saraereh OA, Al Saraira AA, Alsafasfeh QH, et al. (2016) Bio-Inspired Algorithms Applied on Microstrip Patch Antennas: a Review. *International Journal on Communications Antenna and Propagation* 6: 336–347. https://doi.org/10.15866/irecap.v6i6.9737

11. Anguera J, Andújar A, Jayasinghe J, et al. (2016) Nature-Inspired High-Directivity Microstrip Antennas: Fractals and Genetics. In *8th International Conference on Computational Intelligence and Communication Networks*, 204–207. https://doi.org/10.1109/CICN.2016.46

12. Singh G, Singh U (2021) Triple band-notched UWB antenna design using a novel hybrid optimization technique based on DE and NMR algorithms. *Expert Syst Appl* 184: 1–20. https://doi.org/10.1016/j.eswa.2021.115299

13. Mishra RJ, Mishra R, Kuchhal P, et al. (2018) Analysis of the Microstrip Patch Antenna designed using Genetic Algorithm based Optimization for Wide-Band Applications. *International Journal of Pure and Applied Mathematics* 118: 841–849.

14. Lv Y, Cao F, Feng X, et al. (2021)Improved Binary Particle Swarm Optimization and Its Application to Beamforming of Planar Antenna Arrays. *Progress In Electromagnetics Research C* 114: 217–231. https://doi.org/10.2528/PIERC21062002

15. Jabire AH, Abdu A, Salisu S (2017) Multiband Millimeter wave T-shaped antenna with optimized patch parameter using Particle Swarm Optimization. *Nigerian Journal of Technology* 36: 904–909. https://doi.org/10.4314/njt.v36i3.33

16. Jarufe C, Rodriguez R, Tapia V, et al. (2018) Optimized corrugated tapered slot antenna for mm-Wave applications. *IEEE T Antenn Propag* 66: 1227–1235. https://doi.org/10.1109/TAP.2018.2797534

17. Orankitanun T, Yaowiwat S (2020) Application of Genetic Algorithm in Tri-band U-slot Microstrip Antenna Design. In *17th International Conference on Electrical Engineering/Electronics, Computer, Telecommunications and Information Technology (ECTI-CON)*, 127–130. https://doi.org/10.1109/ECTI-CON49241.2020.9158066

18. Lamsalli M, El Hamichi A, Boussouis M, et al. (2016) Genetic Algorithm Optimization for Microstrip Patch Antenna Miniaturization. *Progress In Electromagnetics Research Letters* 60: 113–120. https://doi.org/10.2528/PIERL16041907

19. Jain P, Maheshwari V, Thakre VV (2016) Microstrip Patch Antenna Optimization Using Gentic Algorithm. *International Journal of Engineering Applied Sciences and Technology* 2: 30–33.

20. Venkateshkumar U, Kiruthiga S, Mihitha H, et al. (2020) Multiband Patch Antenna Design for 5G Applications. In *4th International Conference on Computing Methodologies and Communication (ICCMC 2020)*, 528–534. https://doi.org/10.1109/ICCMC48092.2020.ICCMC-00098

21. Kumar R, Kartikeyan MV (2019) Design and Simulation of Multi Band Compact Microstrip Patch Antenna. In *2019 IEEE Indian Conference on Antennas and Propogation (InCAP)*, 1–4.

22. Hussain W, irfan Khattak M, Khattak MA (2020) Multiband Microstrip Patch Antenna for 5G Wireless Communication. *International Journal of Engineering Works* 7: 15–21. https://doi.org/10.34259/ijew.20.7011521

23. Khattak MI, Sohail A, Khan U, et al. (2019) Elliptical Slot Circular Patch Antenna Array with Dual

Band Behaviour for Future 5G Mobile Communication Networks. *Progress In Electromagnetics Research C* 89: 133–147. https://doi.org/10.2528/PIERC18101401

24. Punith S, Praveenkumar SK, Jugale AA, et al. (2020) A Novel Multiband Microstrip Patch Antenna for 5G Communications. *Procedia Computer Science*, 171: 2080–2086. https://doi.org/10.1016/j.procs.2020.04.224
25. Ashraf N, Haraz OM, Ali MM, et al. (2016) Optimized broadband and dual-band printed slot antennas for future millimeter wave mobile communication. *AEU-Int J Electron C* 70: 257–264. https://doi.org/10.1016/j.aeue.2015.12.005
26. Jayasinghe J, Uduwawala DN (2013) Optimization of the performance of patch antennas using genetic algorithms. *J Natl Sci Found Sri* 41. https://doi.org/10.4038/jnsfsr.v41i2.5705
27. Balanis CA (2013) *Modern Antenna Handbook*. A JOHN WILEY and SONS INC, Canada.
28. Dejen A, Anguera J, Ridwan M, et al. (2020) Genetically Engineered Dual-band Microstrip Antenna with Improved Directivity for 5G mm-wave Mobile Applications. In *1st International Women in Engineering Symposium*.
29. Anab M, Khattak MI, Owais SM, et al. (2020) Design and Analysis of Millimeter Wave Dielectric Resonator Antenna for 5G Wireless Communication Systems. *Progress In Electromagnetics Research C* 98: 239–255. https://doi.org/10.2528/PIERC19102404
30. Goldgerg DE (1989) *Genetic Algorithm in Search, Optimization and Machine Learning*. Addison -Wesley Publishing Company Inc., USA.

AIMS Press